Synthesis and Reactivity of Heterodinuclear Fe−Ni Complexes with a Bridging Alkoxysilyl Ligand. Crystal Structure of [(OC)$_3$Fe{μ-Si(OMe)$_2$(OMe)}(μ-dppm)NiMe]†

Pierre Braunstein,* Guislaine Clerc, and Xavier Morise

Laboratoire de Chimie de Coordination, UMR CNRS 7513, Université Louis Pasteur, 4 rue Blaise Pascal, F-67070 Strasbourg Cedex, France

Received July 10, 2001

The new heterobimetallic complex [(OC)$_3$Fe{μ-Si(OMe)$_2$(OMe)}(μ-dppm)NiCl] (**1**) was obtained in 95% yield by reaction of [NiCl$_2$(PPh$_3$)$_2$] in THF with K[Fe{Si(OMe)$_3$}(CO)$_3$(dppm-*P*)] at −78 °C. The analogous bromo and iodo complexes were also obtained; the latter is, however, less stable and could not be isolated pure. They display the first examples of a bridging alkoxysilyl ligand between Fe and Ni, and the μ_2-η^2-SiO bridge is also present in the methyl complex [(OC)$_3$Fe{μ-Si(OMe)$_2$(OMe)}(μ-dppm)NiMe] (**4**) and its phenyl analogue **5**. The presence of the Fe−Si−O→Ni four-membered rings was confirmed by a crystal structure determination of **4**. Treatment of **1** with excess (allyl)MgCl led to the expected bimetallic allyl complex [(OC)$_3${(MeO)$_3$Si}Fe(μ-dppm)Ni(η^3-C$_3$H$_5$)] (**6**). The rapid η^3-allyl → η^1-allyl → η^3-allyl rearrangement is potentially assisted through stabilization of the coordinatively unsaturated Ni center by a SiO→Ni interaction. The bimetallic benzyl derivative **7** was also isolated. Purging a THF or benzene solution of **4** at room temperature with CO yielded after a few seconds the acyl complex [(OC)$_3$Fe{μ-Si(OMe)$_2$(OMe)}(μ-dppm)-NiC(O)Me] (**8**), which readily decarbonylates. Its reaction with norbornadiene leads to the insertion product, which is thought to exist as an isomeric mixture with terminal or chelating acyl group (**11** ⇌ **11′**). When complex **4** was reacted with ^{t}BuNC, rapid insertion occurred and further coordination of a terminal ^{t}BuNC ligand to Ni led to the iminoacyl complex [(OC)$_3${(MeO)$_3$Si}Fe(μ-dppm)Ni{C(N^{t}Bu)Me}(CN^{t}Bu)] (**12**). Complex **1** proved to be a more efficient catalyst (TON = 4100) for the dehydrogenative coupling of Ph$_3$SnH than its mononuclear counterpart [NiCl$_2$(PPh$_3$)$_2$] (TON = 1050). The maximum turnover frequency (TOF) was ca. 9800 h^{-1}.

Introduction

The growing interest in both heterometallic chemistry[1−4] and organosilicon chemistry has led us to investigate new aspects of heterobimetallic silicon chemistry, and a unique interplay between the bimetallic core and the silicon-based ligand was observed in a number of molecules.[5−7] We have concentrated on iron-containing bimetallics, in part because the required iron−silyl precursor is readily available.[6,8] The discovery that a trialkoxysilyl ligand can bridge between two metal centers has opened the way to reactivity studies based on the often-observed lability of the dative O→M bond in the resulting four-membered Fe−Si−O→M ring (Scheme 1).[6,9] The resulting hemilability[10] of the −Si(OR)$_3$ ligand is most pronounced in the case where M = Pd, and we have investigated with such compounds the multiinsertion of organic isonitriles, the sequential

† Dedicated to Professor F. Mathey, on the occasion of his 60th birthday, with our most sincere congratulations and best wishes.

(1) Chetcuti, M. J. In *Comprehensive Organometallic Chemistry II*; Abel, E. W., Stone, F. G. A., Wilkinson, G., Eds.; Pergamon: Oxford, U.K., 1995; Vol. 10, p 23.

(2) Braunstein, P.; Rosé, J. Catalysis and Related Reactions with Compounds containing Heteronuclear Metal−Metal Bonds. In *Comprehensive Organometallic Chemistry II*; Abel, E. W., Stone, F. G. A., Wilkinson, G., Eds.; Pergamon: Oxford, U.K., 1995; Vol. 10, p 351.

(3) Braunstein, P.; Rosé, J. Heterometallic Clusters for Heterogeneous Catalysis. In *Catalysis by Di- and Polynuclear Metal Cluster Complexes*; Adams, R. D., Cotton, F. A., Eds.; Wiley-VCH: New York, 1998; p 443.

(4) Braunstein, P.; Rosé, J. Heterometallic Clusters in Catalysis. In *Metal Clusters in Chemistry*; Braunstein, P., Oro, L. A., Raithby, P. R., Eds.; Wiley-VCH: Weinheim, Germany, 1999; Vol. 2, p 616.

(5) Braunstein, P.; Knorr, M. *J. Organomet. Chem.* **1995**, *500*, 21.

(6) Braunstein, P.; Knorr, M.; Stern, C. *Coord. Chem. Rev.* **1998**, *178−180*, 903.

(7) Braunstein, P.; Knorr, M.; Reinhard, G.; Schubert, U.; Stährfeldt, T. *Chem. Eur. J.* **2000**, *6*, 4265.

(8) Braunstein, P.; Knorr, M.; Schubert, U.; Lanfranchi, M.; Tiripicchio, A. *J. Chem. Soc., Dalton Trans.* **1991**, 1507.

(9) Braunstein, P.; Knorr, M.; Tiripicchio, A.; Tiripicchio-Camellini, M. *Angew. Chem., Int. Ed. Engl.* **1989**, *28*, 1361.

(10) Braunstein, P.; Naud, F. *Angew. Chem., Int. Ed.* **2001**, *40*, 680.

10.1021/om010619p CCC: $20.00
Publication on Web 10/20/2001

Scheme 1

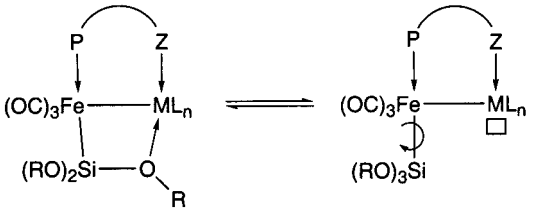

CO/olefin coupling which leads to perfectly alternating polyketones,[11,12] and the catalytic dehydrogenative coupling of stannanes.[13−16] These studies were facilitated by the fact that complexes such as [(OC)$_3$Fe{μ-Si(OMe)$_2$-(OMe)}(μ-dppm)PdX] (dppm = $Ph_2PCH_2PPh_2$; X = Me, Cl, ...) are both stable, largely because of the presence of the bridging diphosphine ligand, and reactive, owing to the kinetic lability of the dative SiO→Pd interaction (Scheme 1).

We have also prepared related Fe−Pt complexes and observed that the lability of the Fe−Si−O→Pt four-membered ring is considerably reduced.[17−20] It became then particularly interesting to investigate the synthesis of heterobimetallic Fe−Ni complexes containing a bridging alkoxysilyl ligand and compare their reactivity with that of their Pd and Pt analogues.

Results and Discussion

1. Synthesis of Fe−Ni Complexes. 1.1. Halide Complexes. The new complex [(OC)$_3$Fe{μ-Si(OMe)$_2$-(OMe)}(μ-dppm)NiCl] (**1**) was prepared by reaction of [$NiCl_2(PPh_3)_2$] in THF with the potassium salt of the silyliron metalate [Fe{Si(OMe)$_3$}(CO)$_3$(dppm-*P*)]$^-$ [8] (in a 1:1 molar ratio) (eq 1). Although **1** is stable for weeks in the solid state under an inert atmosphere, it decomposes upon exposure to air or in solution at room temperature. Thus, to minimize the formation of side products, such as [Ni(CO)$_2$(dppm-*P*,*P*′)],[21] the reaction was carried out at −78 °C and the temperature maintained below 0 °C during workup (see Experimental Section). Under these conditions **1** could be isolated as a green solid in 95% yield.

The analogous bromo complex **2** was similarly prepared from [$NiBr_2(PPh_3)_2$], but in only 40% isolated yield, whereas the iodo derivative **3** was not obtained by reacting the iron metalate with [$NiI_2(PPh_3)_2$]. However, it formed when **1** was reacted with NaI (eq 1). Unfortunately, complex **3** could not be isolated pure, owing to the occurrence of decomposition products during halide metathesis. The spectroscopic and analytical data for **1**−**3** are in agreement with the proposed structure (see Experimental Section and Table 1). In particular, the room-temperature ^{1}H NMR spectra contain for the methoxy protons two singlets in the range δ 3.70−3.68 and 3.26−3.54, in a 2:1 ratio, indicating the presence of a μ_2-η^2-SiO bridge between the Fe and Ni atoms and a static situation on the NMR time scale at room temperature for the silyl ligand. This is in contrast to the observations made with the analogous Fe−Pd complex, where a dynamic situation is observed at room temperature which exchanges the OMe groups.[9] Increasing the temperature led to decomposition of the Fe−Ni complex **1** before coalescence of these resonances could be reached. The ^{31}P{^{1}H} NMR spectra of **1**−**3** show the expected AX pattern for the Fe- and Ni-bound P atoms with a $^{2+3}J_{PP}$ value of ca. 70 Hz (Table 1). This value is in the range of those observed for other Fe(μ-dppm)Pd complexes presenting a SiO→M interaction (M = Pd, Pt, Rh, etc.), whereas in its absence, $^{2+3}J_{PP}$ values larger than 100 Hz are generally observed.[6,22,23] Although many parameters contribute to the ^{31}P NMR chemical shift, we note that changing the nature of the halide ligand on the Ni center induces an important variation of the chemical shift value of the Ni-bound P atom, whereas that of the Fe-bound P atom is unaffected. Thus, on going from X = Cl to X = I, a deshielding is observed (δ 9.4 for **1** vs δ 20.9 for **3**). An opposite but less pronounced trend was noticed for the Pd-bound P atom in related Fe−Pd complexes (δ 34.9 for Fe−Pd−Cl[9] vs δ 32.4 for Fe−Pd−I[24]). In general, complexes **1**−**3** appear less stable than their Pd and Pt analogues, both in the solid state and in solution. This is likely to be due to a weaker metal−metal bond

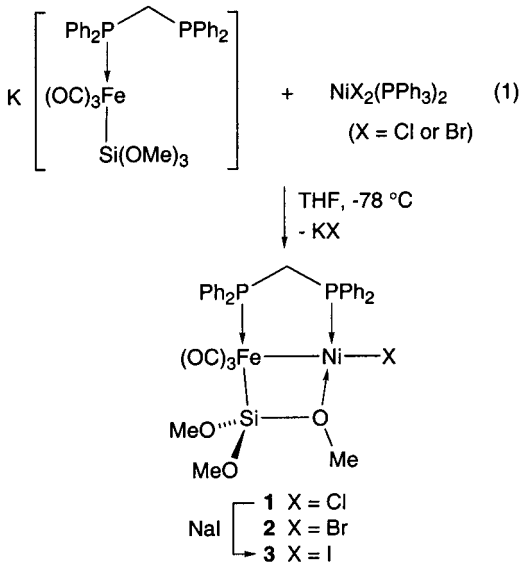

(11) Braunstein, P.; Knorr, M.; Stährfeldt, T. *J. Chem. Soc., Chem. Commun*. **1994**, 1913.
(12) Braunstein, P.; Cossy, J.; Knorr, M.; Strohmann, C.; Vogel, P. *New J. Chem*. **1999**, *23*, 1215.
(13) Braunstein, P.; Morise, X.; Blin, J. *J. Chem. Soc., Chem. Commun*. **1995**, *14*, 1455.
(14) Braunstein, P.; Morise, X. *Organometallics* **1998**, *17*, 540.
(15) Braunstein, P.; Durand, J.; Morise, X.; Tiripicchio, A.; Ugozzoli, F. *Organometallics* **2000**, *19*, 444.
(16) Braunstein, P.; Morise, X. *Chem. Rev*. **2000**, *100*, 3541.
(17) Knorr, M.; Faure, T.; Braunstein, P. *J. Organomet. Chem*. **1993**, *447*, C4.
(18) Knorr, M.; Braunstein, P.; Tiripicchio, A.; Ugozzoli, F. *Organometallics* **1995**, *14*, 4910.
(19) Knorr, M.; Braunstein, P.; DeCian, A.; Fischer, J. *Organometallics* **1995**, *14*, 1302.
(20) Braunstein, P.; Faure, T.; Knorr, M.; Stährfeldt, T.; DeCian, A.; Fischer, J. *Gazz. Chim. Ital*. **1995**, *125*, 35.
(21) van Hecke, G. R.; Horrocks, W. D. *Inorg. Chem*. **1966**, *5*, 1960.
(22) Braunstein, P.; Knorr, M.; Piana, H.; Schubert, U. *Organometallics* **1991**, *10*, 828.
(23) Braunstein, P.; Faure, T.; Knorr, M.; Balegroune, F.; Grandjean, D. *J. Organomet. Chem*. **1993**, *462*, 271.
(24) Balegroune, F.; Braunstein, P.; Durand, J.; Faure, T.; Grandjean, D.; Knorr, M.; Lanfranchi, M.; Massera, C.; Morise, X. Tiripichhio, A. *Monatsh. Chem*. **2001**, *132*, 885.

Table 1. Selected $^{31}P\{^1H\}$ NMR and IR Data of Complexes 1−12

complex	$\delta(^{31}P)$ (ppm)[a] P_{Fe}	P_{Ni}	$^{2+3}J_{pp}$ (Hz)	ν(CO), ν(CN) (cm^{-1})[b]
1	55.3	9.4	72	1982 s, 1931 vs, 1895 s
2	53.8	13.0	71	1983 s, 1932 vs, 1897 s
3	52.1	20.9	70	1986 vs, 1936 vs, 1895 s[d]
4	64.9	32.9	65	1955 s, 1892 vs, 1857 vs
	65.0[c]	33.9[c]	65	
5	62.5	26.3	66	1959 s, 1896 s, 1855 vs
6	71.6[c]	29.7[c]	117	1951 s, 1881 s, 1849 vs
7	62.1	27.3	64	1955 s, 1895 vs, 1858 s
8	65.8	28.3	67	1957 m, 1891 s, 1854 s, 1660 m[d]
11	60.5[e]	28.5[e]	67	1955 s, 1893 vs, 1857 vs, 1717 mw, 1653 mw
12	70.5	37.6	102	2148 m,[f] 1987 s, 1868 m, 1832 m, 1675 w[d,g]

[a] Recorded in C_6D_6 unless otherwise stated. [b] Recorded in THF unless otherwise stated. [c] Recorded in acetone-d_6. [d] Recorded in CH_2Cl_2. [e] Recorded in toluene-d_8. [f] ν(C≡N). [g] ν(C=N).

strength, as usually observed for metal−metal bonds between first-row elements, which is not fully compensated by the SiO→Ni interaction, expected to be stronger than the SiO→Pd and SiO→Pt interactions, owing to the harder character of Ni(II) vs Pd(II) and Pt(II).

1.2. Hydrocarbyl Complexes. To access Fe−Ni complexes containing a Ni−carbon bond, which would allow further reactivity studies, we reacted **1** with MeLi in THF at −78 °C and isolated [(OC)$_3$Fe{μ-Si(OMe)$_2$-(OMe)}(μ-dppm)NiMe] (**4**) in 40% yield (eq 2). The ^{1}H

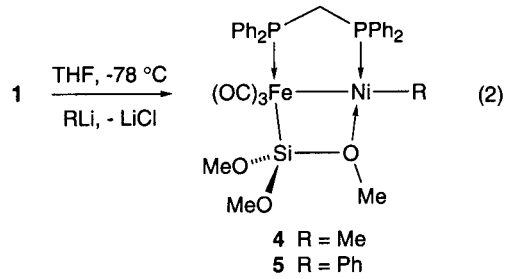

(2)

NMR spectrum of **4** contains a resonance at δ −0.22 ($^3J_{PH}$ = 3.8 Hz) for the Ni methyl protons and two resonances at δ 3.70 and 3.27 for the methoxy protons, in a 2:1 ratio, respectively. This is indicative of the persistence of the SiO bridge present in **1**. The $^{31}P\{^1H\}$ NMR spectrum shows two doublets at δ 64.9 and 32.9 ($^{2+3}J_{PP}$ = 65 Hz), ascribed to the P(Fe) and P(Ni) atoms, respectively. Although crystals of **4** are stable for a few days at −20 °C, noncrystalline solid **4** rapidly decomposed, even at low temperature.

Since complexes **1**−**4** contain the first examples of Fe−Si−O→Ni four-membered rings, a crystal structure determination was performed on **4**. An ORTEP view is shown in Figure 1.

There are two crystallographically different but very similar molecules in the unit cell, whose selected bond distances and angles are given in Tables 2 and 3. Crystal data and data collection parameters are given in Table 4. The Fe and Ni atoms are connected via a direct metal−metal bond, and the Fe−Ni bond lengths of 2.5597(5) Å (in molecule 1) and 2.5688(4) Å (in molecule 2) are comparable to those in other complexes

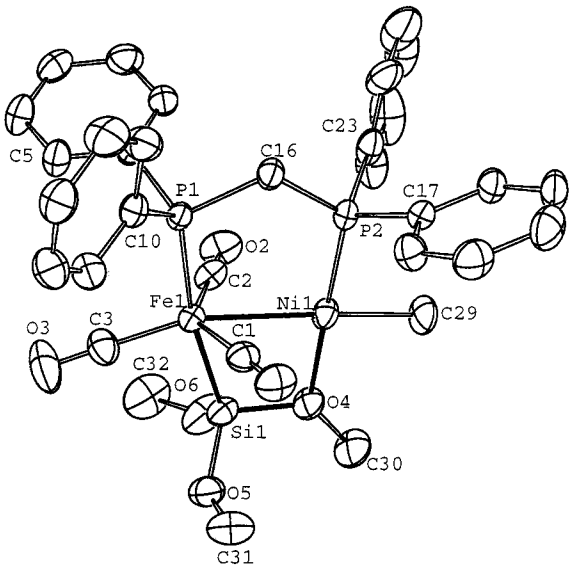

Figure 1. ORTEP view of the structure of [(OC)$_3$Fe{μ-Si(OMe)$_2$(OMe)}(μ-dppm)NiMe] (**4**).

Table 2. Selected Bond Distances (Å) and Angles (deg) in 4 (Molecule 1)

Fe1−Ni1	2.5597(5)	C1−O1	1.163 (3)
Fe1−C1	1.756 (3)	C3−O3	1.153(4)
Fe1−C2	1.767(3)	P1−C16	1.850(2)
Fe1−C3	1.759(3)	P2−C16	1.844(2)
Fe1−P1	2.2098(7)	O4−C30	1.440(3)
Fe1−Si1	2.2558(8)	Si1−O4	1.687(2)
Ni1−P2	2.1020(7)	Si1−O5	1.633(2)
Ni1−C29	1.953(3)	Si1−O6	1.636(2)
Ni1−O4	1.978(2)	O5−C31	1.409(4)
		O6−C32	1.394(4)
Ni1−Fe1−C1	64.83(9)	Fe1−Ni1−P2	97.29(2)
Ni1−Fe1−C2	71.35(9)	Fe1−Ni1−C29	175.38(9)
Ni1−Fe1−C3	162.6(1)	Fe1−Ni1−O4	83.63(6)
Ni1−Fe1−P1	97.48(2)	C1−Ni1−P2	94.99(6)
Ni1−Fe1−Si1	72.75(2)	P2−Ni1−C29	86.92(9)
C1−Fe1−C2	136.1(1)	P2−Ni1−O4	178.50(6)
C1−Fe1−C3	113.0(1)	C29−Ni1−O4	92.2(1)
C2−Fe1−C3	109.8(1)	Fe1−C1−O1	176.6(3)
C1−Fe1−Si1	85.58(9)	Fe1−C2−O2	178.9(3)
C1−Fe1−P1	90.69(8)	P1−C16−P2	115.1(1)
C2−Fe1−P1	91.87(9)	Ni1−O4−C30	132.7(2)
C2−Fe1−S1	84.62(9)	Ni1−O4−Si1	102.61(9)
C3−Fe1−P1	99.8(1)	C30−O4−Si1	124.4(2)
C3−Fe1−Sil	90.0(1)	Fe1−Si1−O4	88.282
P1−Fe1−Si1	170.22(3)		

containing this bond, such as [(OC)$_3$(Me$_3$P)Fe(μ-P^{t}Bu$_2$)-Ni(PMe$_3$)Cl] (Fe−Ni = 2.521 Å).[25] In both molecules the five-membered ring involving the dppm ligand and the Fe and Ni atoms are almost coplanar with the Fe−Si−O→Ni four-membered ring; the dihedral angles between their mean planes is 176.36(3)° (molecule 1) and 175.14(3)° (molecule 2). The Si−O bond involved in the μ_2-η^2-SiO interaction is slightly longer than the other two (Tables 2 and 3). A similar lengthening has been observed in all the previous structural determinations of Fe−Si−O→M systems.[6] The distorted-trigonal-bipy-

(25) Arif, A. M.; Chandler, D. J.; James, R. A. *J. Coord. Chem.* **1988**, *17*, 45.

Table 3. Selected Bond Distances (Å) and Angles (deg) in 4 (Molecule 2)

Fe2−Ni2	2.5688(4)	C33−O7	1.164(3)
Fe2−C33	1.766(3)	C35−O9	1.151(4)
Fe2−C34	1.777(3)	P3−C48	1.846(3)
Fe2−C35	1.767(3)	P4−C49	1.832(3)
Fe2−P3	2.2077(7)	O10−C62	1.437(3)
Fe2−Si2	2.2438(7)	Si2−O10	1.687(2)
Ni2−P4	2.1005(7)	Si2−O11	1.647(2)
Ni2−C61	1.954(3)	Si2−O12	1.638(2)
Ni2−O10	1.982(2)	O11−C63	1.410(3)
		O12−C64	1.433(4)
Ni2−Fe2−C33	65.06(8)	Fe2−Ni2−P4	97.12(2)
Ni2−Fe2−C34	72.90(9)	Fe2−Ni2−C61	175.65(7)
Ni2−Fe2−C35	161.12(9)	Fe2−Ni2−O10	83.64(5)
Ni2−Fe2−P3	97.62(2)	C33−Ni2−P4	96.33(6)
Ni2−Fe2−Si2	72.15(2)	P4−Ni2−C61	87.23(7)
C33−Fe2−C34	137.9(1)	P4−Ni2−O10	178.20(6)
C33−Fe2−C35	110.8(1)	C33−Ni2−O10	83.16(8)
C34−Fe2−C35	109.8(1)	Fe2−C33−O7	176.3(2)
C33−Fe2−Si2	85.73(8)	Fe2−C34−O8	178.5(3)
C34−Fe2−P3	91.51(8)	P3−C48−P4	115.8(1)
C35−Fe2−P3	100.94(9)	Ni2−O10−C62	132.9(2)
C34−Fe2−Si2	83.86(9)	Ni2−O10−Si2	101.41(8)
C33−Fe2−P3	91.58(8)	C62−O10−Si2	125.1(2)
C35−Fe2−Si2	89.38(9)(1)	Fe2−Si2−O10	88.272
P3−Fe2−Si2	169.62(3)		

Table 4. Crystal Data and Data Collection Parameters for 4

formula	$C_{32}H_{34}FeNiO_6P_2Si$
mol wt	719.22
color	orange
cryst syst	monoclinic
a (Å)	15.4860(3)
b (Å)	19.9810(3)
c (Å)	102.620(1)
β (deg)	21.2070(3)
V (Å^3)	6403.5(3)
Z	8
D_{calcd} (g cm^{-3})	1.49
wavelength (Å)	0.710 73
μ (mm^{-1})	1.221
space group	$P2_1/n$
temp (K)	173
radiation	Mo Kα, graphite monochromated
diffractometer	KappaCCD
hkl limits	0−23, 0−29, −32 to +30
θ limits (deg)	2.5−33.69
F(000)	2976
no. of data measd	50 780
no. of data ($I > 3\sigma(I)$)	13 449
weighting scheme	$4F_o^2/(\sigma^2(F_o^2) + 0.0064F_o^4)$
R^a	0.043
$R_w{}^a$	0.065
GOF	1.212
largest peak in final diff map (e Å^{-3})	0.614

[a] $R = \sum||F_o| - |F_c||/\sum|F_o|$; $R_w = [\sum w(|F_o| - |F_c|)^2/\sum w(|F_o|^2]^{1/2}$.

ramidal arrangement of the ligands around the Fe center, when the metal−metal bond is omitted, is also consistent with previous structures and suggests the presence of a formally zerovalent Fe center in these complexes. The Ni(1)−C(1) (molecule 1) and Ni(2)−C(33) (molecule 2) distances of 2.411(3) and 2.427(3) Å are too long for semibridging carbonyl ligands. The Ni−Me distances of 1.953(3) Å (in molecule 1) and 1.954(3) Å (in molecule 2), for which, to the best of our knowledge (CSD search), there is no precedent in a heterobimetallic environment, do not significantly differ from those usually observed in mononuclear systems such as [NiMe(acac)(PCy_3)] (1.941(7) Å)[26] and [NiMe(OPh)-(PMe_3)$_2$] (1.948(1) Å).[27] The Ni−O bond lengths of 1.978(2) Å (in molecule 1) and 1.982(2) Å (in molecule 2) are within the range of those observed in $Na_3(\mu_3$-I)-{Ni[μ_3-OSi(O^{t}Bu)$_3$]$_3$I}·0.5THF·0.5C_5H_{12} (average 1.95 Å)[28] or in Ni(II) cyclohexasiloxanolate sandwich complexes (average value 2.03 Å)[29] and are close to that found in NiO (2.1 Å). They are, however, shorter than the Pd−O and Pt−O bond lengths observed in the related complexes [(OC)$_3$Fe{μ-Si(OMe)$_2$(OMe)}(μ-dppm)-PdCl] (2.100(4) Å)[9] and [(OC)$_3$Fe{μ-Si(OMe)$_2$(OMe)}(μ-dppm)Pt(norbornyl)] (2.217(4) Å),[20] respectively, which is consistent with the smaller radius of Ni(II).

The phenyl analogue of **4**, [(OC)$_3$Fe{μ-Si(OMe)$_2$(OMe)}-(μ-dppm)NiPh] (**5**), was obtained by reaction of **1** with PhLi (eq 2), and its spectroscopic data (see Experimental Section) are similar to those of **4**. It is notable that, although it is stable for several hours in a THF solution, complex **5** could not be isolated pure, owing to rapid decomposition once the solvent is evaporated.

Ni-alkylation reactions using Grignard reagents were also attempted. Thus, treatment of **1** with (allyl)MgCl led to the expected bimetallic allyl complex [(OC)$_3$-{MeO_3Si}Fe(μ-dppm)Ni(η^3-C_3H_5)] (**6**) (Scheme 2). It was characterized by comparison of its NMR data with those of an authentic sample prepared by the better reaction of K[Fe{Si(OMe)$_3$}(CO)$_3$(dppm-*P*)] with [Ni(η^3-allyl)(μ-Cl)]$_2$.[23] Use of an excess of (allyl)MgCl was, however, required in order to achieve complete transformation (^{31}P NMR monitoring). This is probably due to Ni-catalyzed C−C coupling side reactions of allylic fragments.[30] On the basis of the high $^{2+3}J_{PP}$ value of 117 Hz in the ^{31}P{^{1}H} NMR spectrum of **6** (see above) and by analogy with the structure of the Fe−Pd and Fe−Pt analogues of **6**,[22] it is proposed that the allyl ligand adopts an η^3 coordination mode, resulting in the absence of a SiO bridge between the Fe and Ni centers (Scheme 2). However, the presence of broad ^{1}H NMR resonances for the allylic protons suggests the existence in solution of a rapid η^3-allyl → η^1-allyl → η^3-allyl rearrangement potentially assisted through stabilization of the coordinatively unsaturated Ni center by a SiO→Ni interaction (equilibrium **6** ⇌ **6′**, Scheme 2). Low-temperature studies were hampered by poor resolution and solubility problems.[23] Such an allyl $\eta^3 \rightarrow \eta^1 \rightarrow \eta^3$ rearrangement has been investigated in the related Fe−Pd−allyl system.[22] Interestingly, when **1** was treated with 1 equiv of (allyl)MgBr, a mixture of complexes **2** (major product) and **6** was obtained, whereas **2** was the sole product if long reaction times were applied (2 h). This transformation is faster when 2 equiv of (allyl)MgBr is used. Monitoring the reaction by ^{31}P NMR revealed that the

(26) Barnett, B. L.; Kruger, C. *J. Organomet. Chem.* **1972**, *42*, 169.
(27) Kim, Y.-J.; Osakada, K.; Takenaka, A.; Yamamoto, A. *J. Am. Chem. Soc.* **1990**, *112*, 1096.
(28) McMullen, A. K.; Tilley, T. D.; Rheingold, A. L.; Geib, S. J. *Inorg. Chem.* **1990**, *29*, 2228.
(29) Cornia, A.; Fabretti, A. C.; Gatteschi, D.; Pályi, G.; Rentschler, E.; Shchegolikhina, O. I.; Zhdanov, A. A. *Inorg. Chem.* **1995**, *34*, 5383.
(30) Chetcuti, M. J. Nickel−Carbon π-Bonded Complexes. In *Comprehensive Organometallic Chemistry II*; Abel, E. W., Stone, F. G. A., Wilkinson, G., Eds.; Elsevier: Oxford, U.K., 1995; Vol. 9, pp 107, and references therein.

Scheme 2

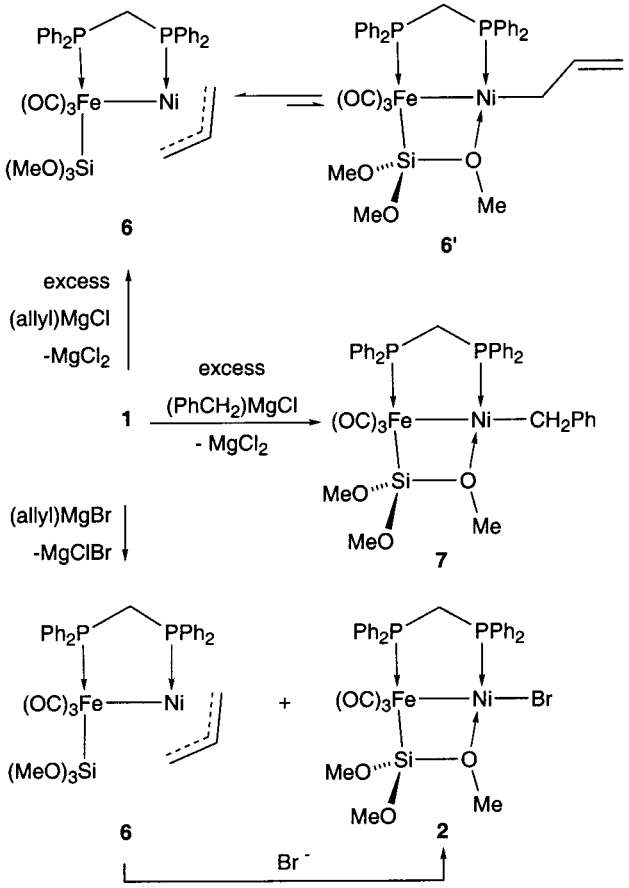

desired product **6** initially forms, together with **2**, and that a rapid decrease of the intensities of its resonances occurs, paralleled by an increase of those of **2**. Since treatment of **1** with (phenyl)MgBr selectively led to the phenyl complex **5**, whereas this latter could not be isolated pure from the reaction of **1** with PhLi, owing to decomposition in the solid state, formation of the bromo complex **2** in the reaction of **1** and (allyl)MgBr certainly results from a displacement of the allyl ligand in **6** by bromide ions, rather than from a direct halide metathesis between **1** and the Grignard reagent (Scheme 2). In agreement with this assumption, we observed the formation of **2** when **1** was reacted with LiBr. In addition, the reaction between **6** and (allyl)MgBr did not afford **2** but the silyliron metalate $[Fe\{Si(OMe)_3\}(CO)_3(dppm\text{-}P)]^-$, as evidenced by $^{31}P\{^1H\}$ NMR spectroscopy (δ 72.8 and −25.8, $^{2+3}J_{PP} = 89$ Hz), formally associated with a $MgBr^+$ cation (which may be solvated). The nickel-containing fragment was not isolated but could be $Ni(allyl)_2$, whose progressive decomposition in solution could account for the formation of 1,5-hexadiene (identified by GC).[31−33] One could therefore envisage that (allyl)MgBr transfers an allyl ligand to **6** with displacement of the Fe−Ni and P→Ni bonds according to eq 3. Note that complex **2** appeared nonreactive toward Grignard or RLi (R = Me, Ph, ...) reagents.

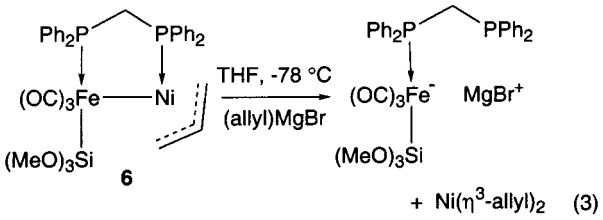

The Ni−benzyl complex **7** was obtained in a manner similar to **6**, from **1** and $(PhCH_2)MgCl$ (Scheme 2). Again an excess of the Grignard reagent was necessary for the reaction to reach completion. Like its Ni−phenyl analogue **5**, complex **7** appeared relatively stable in solution (only ca. 25% decomposition after 24 h in THF, as monitored by ^{31}P NMR) but rapidly decomposed in the absence of solvent, which precluded its isolation in pure form. It was thus characterized in situ by ^{31}P NMR and IR spectroscopic methods. The $^{2+3}J_{PP}$ value of 64 Hz suggests the presence of a SiO→Ni interaction and an η^1 coordination mode for the benzyl ligand (Scheme 2). A similar situation was found for $[(OC)_3Fe\{\mu\text{-}Si(OMe)_2(OMe)\}(\mu\text{-}dppm)PdCH_2Ph]$.[34]

1.3. Spectroscopic Data. Selected spectroscopic data are presented in Table 1, and some have been discussed above. It is perhaps useful to comment briefly on the IR data for the CO ligands. Whereas they are very similar within each of the halide and hydrocarbyl series, a significant shift toward lower wavenumbers is observed on going from the former series to the latter. This would be consistent with the hydrocarbyl ligands being stronger donors than the halides, and we see no other parameter to be invoked, since these molecules are otherwise identical. In the analogous Fe−Pd complexes, we also noticed a significant shift of the ν(CO) values, going from 1995 s, 1940 vs, and 1923 s for $[(OC)_3Fe\{\mu\text{-}Si(OMe)_2(OMe)\}(\mu\text{-}dppm)PdCl]$ (in CH_2Cl_2) to 1956 m, 1892 s, and 1862 vs for the methyl derivative (in CH_2Cl_2).[34] These relatively low ν(CO) values do not imply a semibridging character for the CO ligands, and the X-ray structures of $[(OC)_3Fe\{\mu\text{-}Si(OMe)_2(OMe)\}(\mu\text{-}dppm)PdCl]$[9] and of **4** point toward a terminal bonding mode for these ligands, although weak interactions cannot be completely ruled out. The lower ν(CO) values found in the allyl complex **6** compared to those for **5** or **7** are consistent with the silyl ligand becoming terminal, more electron density remaining with the Fe center. As expected from the formation of the Fe−Ni bond, the ν(CO) values, even in the hydrocarbyl series, remain much higher than in the potassium metalate $K[Fe\{Si(OMe)_3\}(CO)_3(dppm\text{-}P)]$ (1928 w, 1847 vs, 1826 s).[8]

2. Reactions with CO, Norbornadiene, or CN^{t}Bu. Bubling CO through a THF or benzene solution of **4** at room temperature yielded after a few seconds the acyl complex $[(OC)_3Fe\{\mu\text{-}Si(OMe)_2(OMe)\}(\mu\text{-}dppm)NiC(O)$-

(31) Wilke, G.; Bogdanovic, B.; Borner, P.; Breil, H.; Hardt, P.; Heimbach, P.; Herrmann, G.; Kaminsky, H.-J.; Keim, W.; Kröner, M.; Müller, H.; Müller, E. W.; Oberkirch, W.; Schneider, J.; Tanaka, K.; Weyer, K. *Angew. Chem.* **1963**, *75*, 10.
(32) Wilke, G.; Bogdanović, B.; Hardt, P.; Heimbach, P.; Keim, W.; Kröner, M.; Oberkirch, W.; Tanaka, K.; Steinrücke, E.; Walter, D.; Zimmermann, H. *Angew. Chem.* **1966**, *78*, 157−172.
(33) Henc, B.; Jolly, P. W.; Wilke, G.; Benn, R.; Hoffmann, E. G.; Mynott, R.; Schroth, G.; Seevogel, K.; Sekutowski, J. C.; Krüger, C. *J. Organomet. Chem.* **1980**, *191*, 425.
(34) Braunstein, P.; Durand, J.; Kickelbick, G.; Knorr, M.; Morise, X.; Pugin, R.; Tiripicchio, A.; Ugozzoli, F. *J. Chem. Soc., Dalton Trans.* **1999**, 4175.

Scheme 3

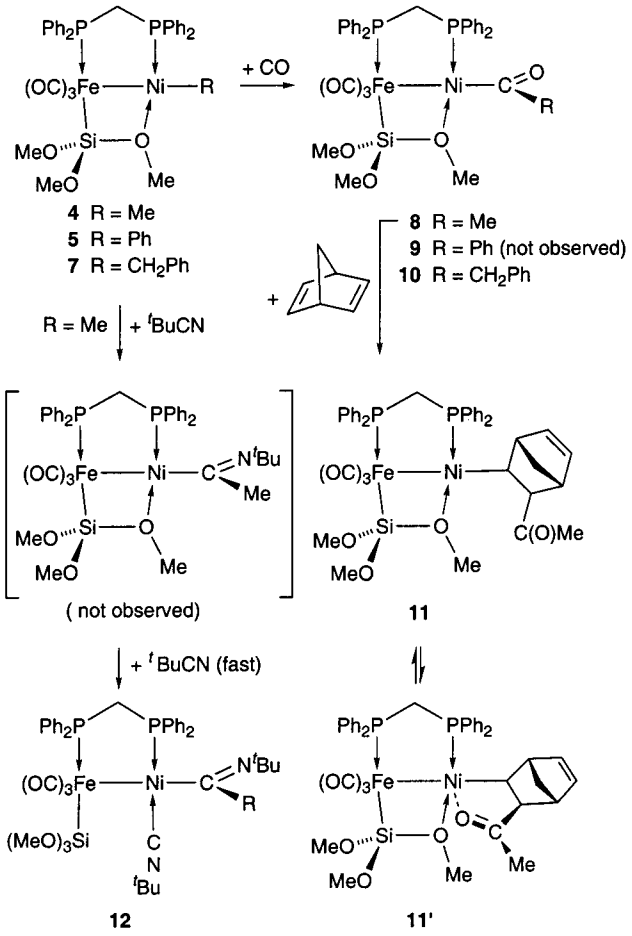

Me] (**8**) (Scheme 3). Insertion of CO into the Ni−Me bond of **4** was evidenced by the occurrence of a ν_{CO} vibration at 1660 cm^{-1}, by a ^1H NMR resonance at δ 1.93 for the acyl protons, and by two new $^{31}P\{^1H\}$ resonances at δ 65.8 and 28.3 ppm ($^{2+3}J_{PP}$ = 67 Hz), which are assigned to the Fe- and Ni-bound P atoms, respectively. Isolation of complex **8** in the solid state was precluded by its tendency to decarbonylate and/or decompose. Note that formation of **8** should be carefully monitored, since it reacts further with CO, leading to decomposition products such as [Ni(CO)$_2$(dppm-*P*,*P*′)].[21] Attempts to carbonylate the phenyl complex **5** did not lead to the benzoyl derivative **9**; however, when **7** was treated with CO (in situ IR monitoring), the complex [(OC)$_3$Fe{μ-Si(OMe)$_2$(OMe)}(μ-dppm)NiC(O)CH$_2$Ph] (**10**) was formed (ν_{CO} 1637 cm^{-1}), which was only observable for a short period of time (Scheme 3).

By analogy with studies on CO/olefin coupling reactions, which led to the addition of the acyl group of the Fe−Pd complex analogous to **8** across the exo face of norbornadiene (NBD),[12] we treated **8** with NBD in THF. IR monitoring showed the disappearance of the ν_{CO} vibration of the acyl group of **8** at 1660 cm^{-1} and the occurrence of new vibrations at 1717 and 1653 cm^{-1}. A new set of two doublets was observed in the $^{31}P\{^1H\}$ NMR spectrum at δ 60.5 and 28.5 ($^{2+3}J_{PP}$ = 67 Hz). The product could not be isolated in pure form, since as already mentionned above for similar complexes, decomposition was observed when volatiles and solvent were evaporated under reduced pressure. On the basis of the IR and $^{31}P\{^1H\}$ NMR spectra and by analogy with previous studies on related Fe−Pd systems,[12] we propose for this new complex the structures pictured in Scheme 3, with the coexistence of a terminal and chelating acyl group (**11** ⇌ **11**′). Attempts to produce polyketones by further reacting either **11**/**11**′ with NBD and CO or **8** with an ethylene/CO mixture (1:1 ratio, 40 bar) were unsuccessful. The high affinity of the Ni center for CO probably accounts for these observations, although Ni(II) complexes have recently been used with success in the copolymerization of ethylene and CO.[35] The rupture of the metal−metal bond of the precursors and formation of mononuclear fragments such as [Ni(CO)$_2$(dppm-*P*,*P*′)][2] and [Fe(CO)$_3$(dppm-*P*,*P*′)] were observed instead.

When complex **4** was reacted with ^{t}BuNC, rapid formation of the iminoacyl complex [(OC)$_3$Fe(μ-dppm)Ni{C(N^{t}Bu)Me}(CN^{t}Bu)] (**12**) was evidenced by the new IR ν_{CN} vibration at 1675 cm^{-1}. An additional vibration at 2148 cm^{-1} is indicative of the presence of a terminal Ni-bound ^{t}BuNC ligand. The $^{31}P\{^1H\}$ NMR spectrum of the new complex consisted of two doublets at δ 70.5 and 37.6, with a $^{2+3}J_{PP}$ coupling of 102 Hz, suggesting the absence of a −SiO bridge between the two metal centers. These data are in favor of the formulation given for complex **12** (Scheme 3). A palladium analogue of this complex has been characterized.[11] Once again, the low stability of the product during workup precluded its isolation in pure form and better characterization.

3. Dehydrogenative Coupling of Ph$_3$SnH. In previous studies we have shown that heterobimetallic alkoxy- and siloxysilyl Fe−Pd complexes were efficient catalysts for the dehydrogenative coupling of stannanes (eq 4).[13−16] It was established that although the elementary chemical transformations take place at the Pd center, the silyl ligand plays a key role in the reaction process, via formation of transient O→Pd interactions. Furthermore, the beneficial effect of the bimetallic structure was demonstrated. Since we are not aware of related catalytic studies with mono- or polynuclear complexes containing nickel,[16] it became of interest to determine the catalytic properties of the Fe−Ni complex **1** for the dehydrogenative coupling of Ph$_3$SnH. Thus, when **1** was added to a Et$_2$O solution of Ph$_3$SnH (ca. 10 000-fold excess; similar reaction conditions were used to determine the catalytic properties of the heterobimetallic silyl Fe−Pd complexes[14−16]), a vigorous evolution of H$_2$ and the formation of Ph$_6$Sn$_2$ were observed. Although its intensity rapidly and continuously decreased, the gas evolution lasted for ca. 2 h. The reaction mixture was, however, stirred for a period of 48 h, to make sure that the reaction went to completion. From the amount of Ph$_6$Sn$_2$ isolated, a turnover number value (TON) of ca. 4100 was determined, whereas unreacted Ph$_3$SnH was recovered. Further runs were carried out during which the evolution of H$_2$ was monitored, and a

$$2Ph_3SnH \xrightarrow{[cat.]} Ph_3Sn{-}SnPh_3 + H_2 \qquad (4)$$

(35) (a) Kläui, W.; Bongards, J.; Rei*β*, G. J. *Angew. Chem., Int. Ed.* **2000**, *39*, 3894. (b) Shultz, C. S.; DeSimone, J. M.; Brookhart, M. **2001**, *20*, 16.

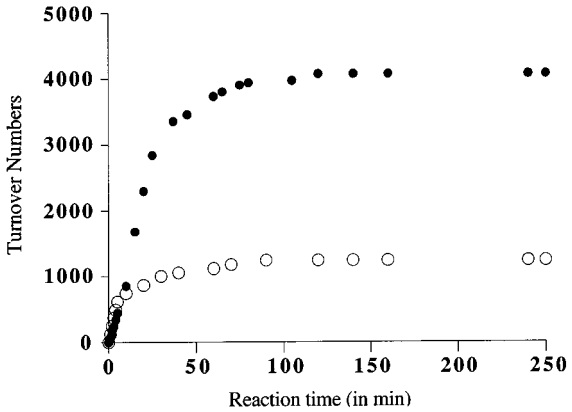

Figure 2. Catalytic dehydrogenative coupling of Ph_3SnH: plot of TON vs time for the complexes **1** and $[NiCl_2(PPh_3)_2]$ (●, Fe−Ni complex **1**; ○, $[NiCl_2(PPh_3)_2]$).

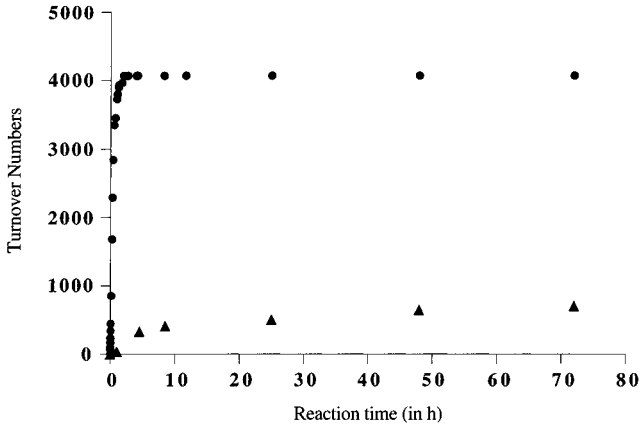

Figure 3. Catalytic dehydrogenative coupling of Ph_3SnH: plot of TON vs time for the complexes Fe−Ni−Cl (**1**) and $[(OC)_3Fe\{\mu\text{-}Si(OMe)_2(OMe)\}(\mu\text{-}dppm)PdCl]$ (●, Fe−Ni complex **1**; ▲, Fe−Pd−Cl complex).

parallel study (under similar reaction conditions) was performed with $[NiCl_2(PPh_3)_2]$ as catalyst (precursor). The comparative data are shown in Figure 2 (●, Fe−Ni complex **1**; ○, $[NiCl_2(PPh_3)_2]$).

The heterobimetallic complex **1** proved to be a more efficient catalyst (TON = 4100) than its mononuclear counterpart $[NiCl_2(PPh_3)_2]$ (TON = 1050). Similar observations have been made for Pd complexes.[14] This reflects a beneficial effect of the bimetallic structure and a positive influence of the Fe fragment on the Ni center, achieved through the metal−metal bonding, the bridging silyl ligand, and the assembling phosphine ligand. Interestingly, when it is compared to its Pd analogue $[(OC)_3Fe\{\mu\text{-}Si(OMe)_2(OMe)\}(\mu\text{-}dppm)PdCl]$ (see Figure 3), complex **1** appears to be a much more efficient catalyst for the dehydrogenative coupling of Ph_3SnH. Not only was a TON value ca. 6 times higher than that observed for obtained but also the time to reach maximum conversion is shortened from ca. 48 h for the Fe−Pd−Cl complex to ca. 2 h for **1**. As a consequence, the maximum turnover frequency (TOF), determined for a given catalyst and expressed in turnovers per hour, found for **1** (ca. 9800 h^{-1}) is much higher than that for the Fe−Pd−Cl complex (ca. 100).[13] Note that when the dehydrogenative coupling of Ph_3SnH catalyzed by **1** was carried out in the presence of a radical scavenger, such as galvinoxyl, the same catalytic performances as in its absence were observed. This is in favor of a nonradical pathway for this reaction. However, its mechanistic details, which probably ressemble those proposed for the Fe−Pd analogous complexes,[14] have not been elucidated. The fate of **1** could not be determined, mainly because of the very small amounts of catalyst employed. The use of **1** as a catalyst for the dehydrogenative coupling of silanes has been unsuccessful so far.

Conclusion

We have shown for the first time that the occurrence of a μ_2-η^2-SiO bridging mode for an alkoxysilyl ligand can be extended to the Fe−Ni couple, as established by the X-ray structure of complex **4**. The nickel halide complexes **1**−**3** are more stable than their analogues containing a Ni−carbon bond, which rapidly decomposed in the solid state and, except for crystalline **4**, were characterized in situ. Insertion reactions of CO, norbornadiene, and ^{t}BuNC into the Ni−C bond of some Fe−Ni heterobimetallic complexes have been observed and were much faster than with the related Fe−Pd complexes. The potential use of these derivatives as catalysts (precursors) for CO/olefins co-oligomerization or polymerization is, however, limited by the formation under CO of Ni-containing side products. However, the dehydrogenative coupling of Ph_3SnH is efficiently catalyzed by complex **1**. Interestingly, the latter proves to be a better catalyst (precursor) than its Fe−Pd analogue. It is also much more efficient than $[NiCl_2(PPh_3)_2]$, which evidences the beneficial effect of the bimetallic structure on the reactivity of the Ni center, through the combined effect of the metal−metal bonding and the assembling diphosphine and bridging alkoxysilyl ligands.

Experimental Section

All the reactions were performed using Schlenk tube techniques under an inert atmosphere of purified nitrogen. Solvents were freshly distilled under nitrogen from the usual drying agent prior to use. Nitrogen was passed through BASF R3-11 catalyst and molecular sieves columns to remove residual oxygen and water. The ^1H and $^{31}P\{^1H\}$ NMR spectra were recorded at 300.13 and 121.5 MHz, respectively, on a FT Bruker AC 300 instrument. Infrared spectra were recorded in the 4000−400 cm^{-1} range on a IFS-66 FTIR Bruker spectrometer and in the 400−90 cm^{-1} range on a IFS-113 FTIR Bruker spectrometer. Samples were prepared as KBr pellets or in solutions using CaF_2 cells.

Synthesis of $[(OC)_3Fe\{\mu\text{-}Si(OMe)_2(OMe)\}(\mu\text{-}dppm)NiCl]$ (1). To a stirred THF solution (10 mL) solution of $[NiCl_2(PPh_3)_2]$ (5.24 g, 8.0 mmol), at −78 °C was added a filtered (Celite pad) THF solution (30 mL) of $K[Fe\{Si(OMe)_3\}(CO)_3(dppm\text{-}P)]$ prepared from $[HFe\{Si(OMe)_3\}(CO)_3(dppm\text{-}P)]$ (5.18 g, 8.0 mmol) and excess KH.[8] After the mixture was stirred for 0.5 h at −78 °C, it was filtered and the volatiles were removed under vacuum at 0 °C, giving a green residue. The latter was washed with pentane (20 mL) and Et_2O (25 mL), affording **1** as a green solid which was dried under vacuum (6.21 g, 95%). ^1H NMR (C_6D_6, 298 K): δ 8.2−6.8 (m, 20H, aromatics); 3.70 (s, 6H, $Si(OMe)_2$); 3.26 (s, 3H, μ-SiOMe); 3.11 (t, 2H, $^2J_{PH}$ = 10 Hz, PCH_2P). IR (polyethylene): ν(NiCl) 336 cm^{-1}. Anal. Calcd for $C_{31}H_{31}ClFeNiO_6P_2Si$: C, 50.34; H, 4.22. Found: C, 50.02; H, 4.44.

Synthesis of [(OC)$_3$Fe{μ-Si(OMe)$_2$(OMe)}(μ-dppm)NiBr] (2). This compound was prepared in a manner similar to **1** from [HFe{Si(OMe)$_3$}(CO)$_3$(dppm-*P*)] (5.185 g, 8.0 mmol) and [NiBr$_2$(PPh$_3$)$_2$] (5.95 g, 8.0 mmol). Complex **2** was isolated as a green solid (2.51 g, 40%). ^{1}H NMR (C_6D_6, 298 K): δ 8.2−6.7 (m, 20H, aromatics); 3.70 (s, 6H, Si(OMe)$_2$); 3.33 (s, 3H, μ-SiOMe); 3.18 (t, 2H, $^2J_{PH}$ = 10 Hz, PCH$_2$P). Anal. Calcd for $C_{31}H_{31}BrFeNiO_6P_2Si$: C, 47.49; H, 3.99. Found: C, 47.27; H, 4.45.

Formation of [(OC)$_3$Fe{μ-Si(OMe)$_2$(OMe)}(μ-dppm)NiI] (3). To a stirred solution of **1** (0.123 g, 0.17 mmol) in THF (20 mL) was added NaI (0.027 g, 0.18 mmol) at room temperature. After the reaction mixture was stirred for 1 h, it was filtered, and the solvent was removed under reduced pressure. The residue was then washed with 10 mL of hexane and 20 mL of Et$_2$O, affording a green-brown solid which was dried under vacuum. ^{1}H NMR (C_6D_6, 298 K): δ 8.2−6.7 (m, 20H, aromatics); 3.68 (s, 6H, Si(OMe)$_2$); 3.54 (s, 3H, μ-SiOMe); 3.28 (t, 2H, $^2J_{PH}$ = 10.1 Hz, PCH$_2$P). Owing to some decomposition, this complex could not be isolated analytically pure.

Synthesis of [(OC)$_3$Fe{μ-Si(OMe)$_2$(OMe)}(μ-dppm)NiMe] (4). To a stirred solution of **1** (1.515 g, 2.05 mmol) in THF (50 mL) at −78 °C was added MeLi (1.6 M) in Et$_2$O (1.34 mL, 2.15 mmol) via a syringe. After completion of the reaction (0.5 h, IR monitoring in the ν_{CO} region) the solvent was evaporated, toluene was added (50 mL), and the mixture was filtered. The filtrate was concentrated to 10 mL, and CH$_2$Cl$_2$ (10 mL) was added slowly. The Schlenk flask was placed at −20 °C, and orange crystals of **4** slowly formed (0.59 g, 40%). ^{1}H NMR (acetone-d_6, 298 K): δ 8.1−6.8 (m, 20H, aromatics); 3.70 (s, 6H, Si(OMe)$_2$); 3.66 (dd, 2H, $^2J_{PH}$ = 11.4, 11 Hz, PCH$_2$P); 3.27 (s, 3H, μ-SiOMe); −0.22 (s, 3H, ^3J(P−H) = 3.8 Hz, NiCH$_3$). Anal. Calcd for $C_{32}H_{34}FeNiO_6P_2SiCH_2Cl_2$: C, 49.29; H, 4.51. Found: C, 49.64, H, 4.55.

Synthesis of [(OC)$_3$Fe{μ-Si(OMe)$_2$(OMe)}(μ-dppm)NiPh] (5). This complex was synthesized in a method similar to **4** using PhLi (1.8 M in cyclohexane/Et$_2$O). Unfortunately, it could not be isolated pure, owing to rapid decomposition in the solid state. However, **5** was unambiguously characterized by spectoscopic methods in solution (THF) and by comparison of its data with those of **4**. ^{1}H NMR (C_6D_6, 298 K): δ 8.1−6.6 (m, 25H, aromatics); 3.47 (s, 6H, Si(OMe)$_2$); 3.33 (br, 2H, PCH$_2$P); 3.10 (s, 3H, μ-SiOMe).

Formation of [(OC)$_3${(MeO)$_3$Si}Fe(μ-dppm)Ni(η^3-C$_3$H$_5$)] (6). To a stirred solution of **1** (0.365 g, 0.49 mmol) in THF at −78 °C was added a 2 M solution of (allyl)MgCl in THF (0.245 mL, 0.49 mmol) via a syringe. The solution immediately turned red. After it was stirred for 2 h at −78 °C, the solution was filtered and concentrated. The ^{31}P{^{1}H} NMR spectrum showed a 1:1 mixture of **6** and unreacted **1**. When more than 2 equiv of (allyl)MgCl was used, only complex **6** was observed. The preparation of **6** was also attempted from **1** and (allyl)MgBr. Under stoichiometric conditions, a 1:1 mixture of **6** and **2** was obtained, whereas when more than 2 equiv of (allyl)MgBr was used, complete transformation to the bromo complex **2** was observed. Complex **6** could not be separated from **1** or **2**, respectively, but it was characterized in situ by ^{31}P{^{1}H} NMR and IR spectroscopy.

Formation of [(OC)$_3$Fe{μ-Si(OMe)$_2$(OMe)}(μ-dppm)NiCH$_2$Ph] (7). This complex was obtained in a manner similar to **6** from (PhCH$_2$)MgCl (2 M in Et$_2$O) (0.90 mL, 1.8 mmol) and **1** (0.4 g, 0.59 mmol) in THF (30 mL). The red mixture was filtered and concentrated to ca. 5 mL, and an aliquot was analyzed by ^{31}P{^{1}H} NMR and IR spectroscopy (Table 1). This complex is unstable in the solid state.

Formation of [(OC)$_3$Fe{μ-Si(OMe)$_2$(OMe)}(μ-dppm)NiC(O)Me] (8). CO was bubbled for a few seconds through a C_6D_6 solution of **4** (0.06 g, 0.084 mmol) at room temperature, until the solution turned deep red. It is then necessary to stop the CO current to prevent decomposition of the acyl complex **8**. ^{1}H NMR (C_6D_6, 298 K): δ 8.0−6.6 (m, 20H, aromatics); 1.93 (s, 3H, NiC(O)CH$_3$).

Formation of [(OC)$_3$Fe{Si(OMe)$_3$}(μ-dppm)Ni(CN^{t}Bu){C(Me)=N^{t}Bu}] (12). To a stirred solution of **4** (0.103 g, 0.15 mmol) in CH$_2$Cl$_2$ was added 1 equiv of ^{t}BuNC (0.0125 g) via syringe. The orange solution turned red, and the corresponding complex **12** could only be characterized in situ (see text).

Dehydrogenative Coupling of Ph$_3$SnH Catalyzed by 1 and [NiCl$_2$(PPh$_3$)$_2$]. A Schlenk flask equipped with a stirring bar and a serum cap was charged with Ph$_3$SnH (4.98 g, 14.2 mmol) in 15 mL of Et$_2$O and was placed in a water bath at 293 K. The volume of H$_2$ released was monitored, using the following procedure: the Schlenk was fitted onto a gas buret, and the catalyst (14.2×10^{-4} mmol in 1 mL of Et$_2$O) was rapidly added to the reaction mixture via syringe through the serum cap. The turnover numbers were calculated using the following equation: TON = (*n* mol of H$_2$)/(*n* mol of catalyst), with the number of moles of H$_2$ being determined by applying the gas equation: $PV = nRT$. Each experiment was repeated at least two times, and the mean values were used for the plots. When the reaction was over, after decantation and filtration the residue was washed with Et$_2$O, affording Ph$_6$Sn$_2$ as a white solid (mp 225−235 °C); the ^{1}H NMR spectrum only showed signals in the aromatic region. The turnover numbers determined from the amount of Ph$_6$Sn$_2$ recovered were in all cases in good accordance with those determined from the volumes of H$_2$ released.

Acknowledgment. We are grateful to Dr. M. Knorr for preliminary experiments and discussions and to the CNRS and the Ministère de la Recherche (Paris) for financial support.

Supporting Information Available: Tables of atomic coordinates, anisotropic displacement parameters, and all bond lengths and angles for **4**. This material is available free of charge via the Internet at http://pubs.acs.org.

OM010619P